Check for updates

Received: 12 May 2023 | Revised: 23 November 2023 | Accepted: 20 April 2024

IET Renewable Power Generation

DOI: 10.1049/rpg2.13017

The Institution of Engineering and Technology WILEY

ORIGINAL RESEARCH

An improved regression-based perturb and observation global maximum power point tracker methods

Hasan Gundogdu[1] | Alpaslan Demirci[1] | Said Mirza Tercan[1] | Ali Durusu[1,2]

[1]Department of Electrical Engineering, Yildiz Technical University, Istanbul, Turkey

[2]Clean Energy Technologies Institute, Yildiz Technical University, Istanbul, Turkey

Correspondence
Said Mirza Tercan, Department of Electrical Engineering, Yildiz Technical University, Istanbul 34220, Turkey.
Email: stercan@yildiz.edu.tr

Abstract

Solar photovoltaic energy is a vital renewable resource because it is clean, endless, and pollution-free. Due to the fast growth of the semiconductor and power electronics sectors, photovoltaic (PV) technologies are climbing significant attention in modern electrical power applications. Operating PV energy conversion systems at the maximum power point is essential for getting the maximum power output and raising efficiency. This paper proposes a regression-based Perturb and Observe method to quickly find a global maximum power point, avoiding being stuck in local maxima, likewise analytical and metaheuristic methods. The improved control focuses on the narrowed search areas by linear and non-linear regression analyses using the generated PV model on a flexible Python environment. Furthermore, the method's accuracy is validated in real time under variable temperatures, irradiations, and loads. This method was proven with a hardware implementation. The proposed method is more than 98% accurate and can withstand long-term modelling. The suggested regression-based perturbation and observation method provided a short learning time and easy implementation. Additionally, the dynamic recorded results can be visualized for researchers to utilize efficiently.

1 | INTRODUCTION

The significant increase in energy demand, the recent environmental concerns, and the reserve problem of fossil fuels have led to a tendency towards renewable energy sources (RES). Solar photovoltaic (PV) energy generation is intermittent and variable because of sudden changes in irradiation and temperature. Maximizing efficiency under variable irradiance is a challenging issue for PV systems. Especially, partial shading (PS) due to cloud movements or improper positioning reduces the efficiency and output power [1]. The maximum power point tracker (MPPT) keeps the PV array continuously on maximum power point (MPP) with the help of optimization algorithms [2]. The non-linear nature of PV leads to many local maxima on characteristic curves under PS [3, 4]. There is only one MPP on the characteristic curve under uniform irradiance, as indicated by the red line in Figure 1. However, some local MPPs are on the blue and green lines in Figure 1 due to PS. Among the conventional MPPT algorithms, perturbation & observation (P&O) [5, 6] and incremental conductance [7] are the most widely investigated. The main reasons are their low cost and simplicity with the ability to track MPP under uniform radiation. In contrast, the main drawbacks of these algorithms are oscillations generated around the MPP and insufficiency under PS conditions by falling to the nearest local maximum power point (LMPP). Besides, these classical algorithms are insufficient to track the global maximum power point (GMPP) under non-uniform irradiance [8].

Numerous studies have been performed to track global MPP under several PS conditions using various meta-heuristic optimization algorithms [9]. Particle Swarm Optimization (PSO) is a bio-inspired, intelligence-based meta-heuristic optimization algorithm. The PSO technique performs better than the conventional MPPT methods, which cannot track global MPP (GMPP) under PS conditions [10]. PSO has been extensively used for various engineering applications due to good accuracy, simpler structure, high adaptability, and few tuning parameters. Still, it has drawbacks, like steady-state oscillation, convergence

This is an open access article under the terms of the Creative Commons Attribution-NonCommercial-NoDerivs License, which permits use and distribution in any medium, provided the original work is properly cited, the use is non-commercial and no modifications or adaptations are made.
© 2024 The Author(s). *IET Renewable Power Generation* published by John Wiley & Sons Ltd on behalf of The Institution of Engineering and Technology.

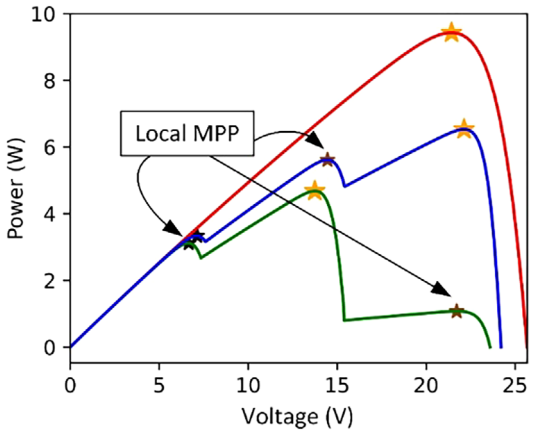


FIGURE 1 Global and local maximum power points.

ability, and tracking speed. Therefore, improving PSO regarding searching speed and reducing oscillation have gained enormous attention from researchers [11, 12]. Harris Hawks optimization (HHO) is proposed by Heidari et al. [13, 14]. HHO has been utilized recently for multiple engineering problems like MPPT algorithms to find the GMPP of a PV array during PS. The advantages of HHO for MPPT are effectively minimizing the undesired steady-state oscillation and high-power conversion efficiency with good accuracy. However, HHO may fall into local maximum points, and it takes longer to find the MPP under the shading conditions. Grey Wolf Optimization (GWO) is a recently emerged bio-inspired swarm-based meta-heuristic optimization algorithm introduced by Mirjalili et al. in 2014 [15]. The GWO gives competitive results compared to popular swarm-based algorithms in terms of accuracy, convergence independency, simple control, and the ability to deal with local minima [16]. Additionally, enhanced GWO was used for the PV system for tracking GMPP under PS, simplifying the calculation process with high accuracy. However, the accuracy and tracking time in the basic GWO can still be further improved for various PS conditions [17]. These methods have significantly reduced tracking time, power losses, and oscillations and enhanced efficiency [18, 19].

On the other hand, soft computing MPPT algorithms, such as artificial intelligence and metaheuristic algorithms, were introduced to address the issues of conventional MPPT techniques [20]. Artificial intelligence methods have been involved in various works to enhance PV performance under PS conditions, such as fuzzy logic control (FLC) [21] and artificial neural network (ANN) [22]. However, such artificial intelligence algorithms are costly, complicated, require long computation time, and need prior knowledge [23]. It is necessary that they avoid falling into local maximum, especially under PS conditions, and can easily be implemented. The complex traditional MPPT techniques poorly locate the GMPP under PS conditions [24–26]. Recently, there have been efforts to combine conventional MPPT methods with meta-heuristic algorithms to effectively track global MPP under PS. Although hybridization has improved the MPPT performance [27], it has disadvantages, such as increased complexity and computational burden [28, 29].

Several studies have recently described different methods for forecasting the MPP of PV, including machine learning methods like regression [30]. The most significant advantage of regression is the forecasting ability based on a small number of statistical samples. Compared to FLC and ANN, it requires a short learning time and easy implementation. The present MPPT methods have limitations, such as difficult implementation and power loss due to rapid duty cycle variations during the tracking. The larger step size of the duty cycle results in more power oscillations, and the small step size affects convergence speed [31]. Most MPPT methods adjust the perturbation step in voltage to overcome the step size drawbacks of P&O. A small voltage step reduces the oscillations around MPP and the power loss. But it slows down the response of the control algorithm to changing atmospheric conditions and decreases efficiency [32]. Thus, implementing linear and non-linear regressions with photovoltaic models (PVM) characteristics to track MPP has been tracked more effectively than P&O and has had similar success to PSO [33]. Also, the linear and non-linear regressions precisely predict the perturbation's step size to improve the tracking performance of MPPT with limited computational difficulty. Therefore, this paper focused on the combination of traditional P&O and regression. The simulations have proved the success of the regression model under uniform irradiation conditions [34]. There is still a lack of proven long-term success and clear effectiveness under non-uniform and real irradiation conditions.

Thus, performance parameters include convergence speed, oscillation reduction, accuracy, and computational time. Fast convergence allows the MPPT algorithm to quickly adjust the MPP under changing environmental conditions [35]. Achieving fast convergence involves selecting an appropriate control strategy and tuning algorithm parameters to respond quickly to changes in irradiance, temperature, and other PV system factors. Designing an effective MPPT algorithm involves techniques to reduce oscillations and ensure stable operation at or near MPP. Accuracy is of the utmost importance in MPPT to ensure that the PV system operates as close as possible to its true MPP. The MPPT algorithm should accurately estimate the MPP under varying environmental conditions and PV characteristics [36]. Properly modelling the PV system requires considering factors such as temperature and shading and using accurate algorithms that can handle different operating conditions. MPPT algorithms have been improved for fast computation time, and efficient MPPT methods must be designed to balance accuracy and response time. Additionally, hardware considerations such as MPPT controller processing power and available resources should be considered to ensure real-time operation. In short, an effective MPPT algorithm should have a fast convergence speed, reduce oscillations around the MPP, achieve high accuracy in estimating the MPP, and maintain an acceptable computational time. The balance between these factors is critical for optimal power harvest, stability, and efficiency of the PV system. Depending on the application, available resources,

17521424, 2024, 9-10, Downloaded from https://ietresearch.onlinelibrary.wiley.com/doi/10.1049/rpg2.13017 by Yildiz Technical University, Wiley Online Library on [19/07/2024]. See the Terms and Conditions (https://onlinelibrary.wiley.com/terms-and-conditions) on Wiley Online Library for rules of use; OA articles are governed by the applicable Creative Commons License

and system requirements, specific design choices and techniques may vary.

This paper proposes a regression-based P&O MPPT method to find GMPP speedily, avoiding being stuck in local MPP. Generated PVMs on a flexible Python environment have been used in linear and non-linear regression analyses. Regression analyses narrowed search areas to improve the speed of finding MPPT for preventing falling into local maxima. Furthermore, the accuracy of results is validated in real time under variable temperatures, irradiations, and loads. This method was proven with hardware implementation under dynamic and long-term experiments. The original contributions of this study are listed as follows:

- Linear and non-linear regressions were derived via the scikit-learn package using MPPs obtained with 5PM.
- Regression methods have enhanced the analytical search algorithm performance for global maximum power point tracker (GMPPT) by narrowing the search areas.
- The proposed method is more than 98% accurate and can withstand long-term modelling.
- The suggested regression-based P&O method provided a short learning time and easy implementation.

This article is organized as follows. Section 2 contains the PV modelling, the methodology, and system descriptions. Section 3 presents experimental performance results and discusses the proposed method's accuracy. Finally, this study concludes in Section 4.

2 | METHODOLOGY AND SYSTEM DESCRIPTIONS

The MPPT controller decides the duty cycle using several algorithms to compute the PV array's measured output voltage and current. PV cells are connected in series or parallel to form a PV module. The PV array consists of many PV modules to obtain the required voltage and current. PV arrays are connected to the loads via a converter. The block diagram PV system is presented in Figure 2.

2.1 | Designing PV models and shading patterns

Researchers have developed PVM using different PV electrical equivalent circuits [37–39]. PV panel manufacturers determine panel characteristics under standard test conditions (STC) as 1000 W/m^2 and 25°C. The most preferred single-diode solar panel equivalent circuit is given in Figure 3, thanks to its success and easy applicability [40–43].

Equation (1) describes the ideal PV panel I–V characteristic. I_{PV} is the current generated according to irradiation, I_0 is diode reverse saturation current, q is electron load ($1.60217646 \times 10^{-19}$ C), n is diode quality factor, k is Boltzmann constant ($1.3806503 \times 10^{-23}$ J/K), T is p–n junction temperature in Kelvin [41].

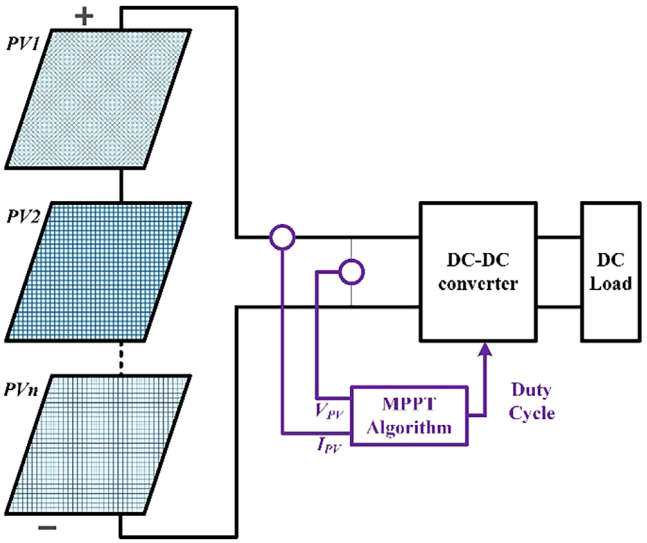


FIGURE 2 The block diagram for the proposed MPPT. MPPT, maximum power point tracker.

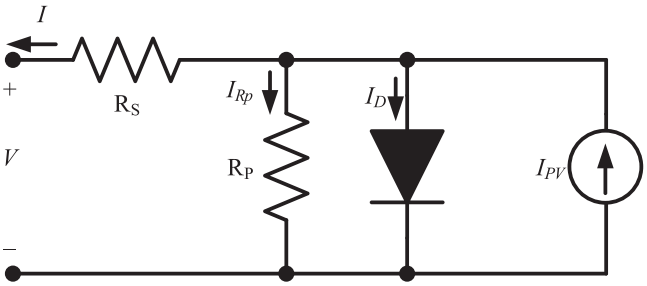


FIGURE 3 Single-diode equivalent circuit.

$$I = I_{PV} - I_D - I_{Rp} \tag{1}$$

$$I_D = I_0 \left[e^{\left(\frac{qV}{nkT}\right)} - 1 \right] \tag{2}$$

$$I_{R_p} = \frac{V + I.R_S}{R_P} \tag{3}$$

Representing real PV cell losses and leakage current, R_s and R_p determine the slope in constant voltage and constant current regions [44]. Several PV models have been proposed presenting I–V characteristics successfully analytically and using meta-heuristically under various weather conditions.

5PM is an analytical technique that uses mathematical equations to find the required solar panel values. An analytical method is rather complicated due to the unprovided parameters of PVM and the I–V non-linearity [45]. However, metaheuristic algorithms and artificial intelligence techniques excel in solving such non-linear problems [46]. Different optimization techniques and metaheuristics have recently been developed to

17521424, 2024, 9-10, Downloaded from https://ietresearch.onlinelibrary.wiley.com/doi/10.1049/rpg2.13017 by Yildiz Technical University, Wiley Online Library on [19/07/2024]. See the Terms and Conditions (https://onlinelibrary.wiley.com/terms-and-conditions) on Wiley Online Library for rules of use; OA articles are governed by the applicable Creative Commons License

calculate solar panel parameters [47, 48]. Ram et al. found the I–V curve using the hybrid Bee Pollinator Flower Algorithm [49]. The developed PVM proved successful even at low irradiance levels and with fewer errors than other algorithms [50]. Derrick et al. found the I–V curve using the Pattern Search algorithm. The model efficiency was tested in MATLAB/Simulink environment at various irradiation and temperature and compared with the experimental data obtained from the PVM, Kyocera – KC200GT 215 panel [51]. As a result, the developed model is quite successful not only in terms of accuracy but also in terms of the I–V curve generation duration. In many studies, it is aimed to obtain optimum results by training ANN with the help of developed heuristic algorithms [52, 53]. This study created the PV model using De Soto-5PM in the Python PVlib library [54].

5PM, developed by De Soto et al., is one of the most widely used analytical methods. I–V characteristic curves are created with these five parameters (I_{PV}, I_0, R_s, R_p, a) of 5PM using Equation (7) [41, 55]. Equation (4) describes PV cell current using factor a determined in Equation (5). N_s is serial cell number, n_I is ideality factor, T_c cell temperature, and k and q as determined in Equation (1).

$$I = I_{PV} - I_0\left[e^{\frac{V+I.R_s}{a}} - 1\right] - \frac{V + I.R_s}{R_p} \tag{4}$$

$$a = \frac{N_s.n_I.k.T_c}{q} \tag{5}$$

The I–V curve of 5PM under STC can be solved for short circuit, maximum power, and open-circuit points using Equations (6) to (8).

Short-circuit point ($I = I_{SC}, V = 0$)

$$I_{SC} = I_{PV} - I_0\left(e^{\frac{I_{SC}.R_s}{a}} - 1\right) - \frac{I_{SC}.R_s}{R_p} \tag{6}$$

Maximum power point ($I = I_{MPP}, V = V_{MPP}$)

$$I_{MPP} = I_{PV} - I_0\left(e^{\frac{V_{MPP}+I_{MPP}.R_s}{a}} - 1\right) - \frac{V_{MPP} + I_{MPP}.R_s}{R_p} \tag{7}$$

Open-circuit point ($I = 0, V = V_{OC}$)

$$I_{PV} - I_0\left(e^{\frac{V_{OC}}{a}} - 1\right) - \frac{V_{OC}}{R_p} = 0 \tag{8}$$

Equation (9) is written since the power derivative at the maximum power point must be zero.

$$\left.\frac{d\,(P)}{d\,(V)}\right|_{MPP} = I_{MPP} - V_{MPP}\left.\frac{dI}{dV}\right|_{MPP} = 0 \tag{9}$$

The temperature coefficient for open circuit is calculated using Equation (10).

$$\mu_{V_{OC}} = \left.\frac{dV}{dT}\right|_{I=0} \approx \frac{V_{OC_{STC}} - V_{OC_{T_c}}}{T_{c_{STC}} - T_c} \tag{10}$$

5PM is solved using the assumptions in Equations (11) to (14). E_g, energy band gap in Equation (12), G is irradiation intensity, and M is air mass in Equation (13).

$$\frac{a}{a_{STC}} = \frac{T_c}{T_{c_{STC}}} \tag{11}$$

$$\frac{I_0}{I_{0_{STC}}} = \left[\frac{T_c}{T_{c_{STC}}}\right]^3 e^{\frac{1}{k}\left[\frac{E_{g_{STC}}}{T_{c_{STC}}} - \frac{E_g}{T_c}\right]} \tag{12}$$

$$I_{PV} = \frac{G}{G_{STC}}\frac{M}{M_{STC}}\left[I_{L_{STC}} + \mu_{I_{sc}}\left(T_c - T_{c_{STC}}\right)\right] \tag{13}$$

$$\frac{R_p}{R_{p_{STC}}} = \frac{G_{STC}}{G} \tag{14}$$

5PM could be calculated with a simpler method with the same precision even in changing weather conditions, proving a 1% error along the I–V curve [38]. R_s and R_p are solved iteratively, but I_L and I_0 are solved using Equations (15) and (16) where n is diode quality factor.

$$0 = I_{PV} - I_0\left(e^{\frac{V_{OC}}{nT}} - 1\right) - \frac{V_{OC}}{R_p} \tag{15}$$

$$I_0 = \frac{\left[I_{SC}\left(1 + \frac{R_s}{R_p}\right) - \frac{V_{OC}}{R_p}\right]}{e^{\frac{V_{OC}}{nT}}} \tag{16}$$

Lo Brano et al. modelled the I–V curve using the trial-and-error method with manufacturer data according to Equation (17). R_s and R_p are considered constant for each irradiation and temperature [56].

$$I\,(\alpha_G, T) = \alpha_G\, I_{PV}\,(T) - I_0\,(\alpha_G, T)\left(e^{(\alpha_G[V+KI\,(T-T_{STC}]+IR_s)/\alpha_G nT} - 1\right) - \frac{\alpha_G\,[V + KI\,(T - T_{STC})] + IR_s}{Rp} \tag{17}$$

Hadj Arab et al. calculated the desired parameters using Equations (18) and (19) with the values provided by the manufacturer ($V_{OC}, I_{SC}, V_{MPP}, I_{MPP}$) [57].

$$R_s = -\left(\frac{dV}{dI}\right)_{V=V_{OC}} \tag{18}$$

$$R_p = -\left(\frac{dV}{dI}\right)_{I=I_{SC}} \tag{19}$$

The error comparison of 5PMs is given in Table 1. Accordingly, Lo Brano's method in [56] is the best regarding mean and total errors.

The uniform and non-uniform irradiance patterns under clear sky (CS), cloudy, and partial cloudy are given in Figure 4. It is assumed that all three modules receive uniform irradiation under CS.

17521424, 2024, 9-10, Downloaded from https://ietresearch.onlinelibrary.wiley.com/doi/10.1049/rpg2.13017 by Yildiz Technical University, Wiley Online Library on [19/07/2024]. See the Terms and Conditions (https://onlinelibrary.wiley.com/terms-and-conditions) on Wiley Online Library for rules of use; OA articles are governed by the applicable Creative Commons License

TABLE 1 The error comparison of 5PMs.

	Mean error					
Irradiation [W/m^2]	**200**	**400**	**600**	**800**	**1000**	**Total error**
Lo Brano [56]	0.41	0.68	1.06	0.4	0.39	0.59
De Blas [58]	1.36	1.87	2.02	1.48	0.39	1.42
Hadj Arab [57]	3.19	4.82	5.01	4.12	0.39	3.51

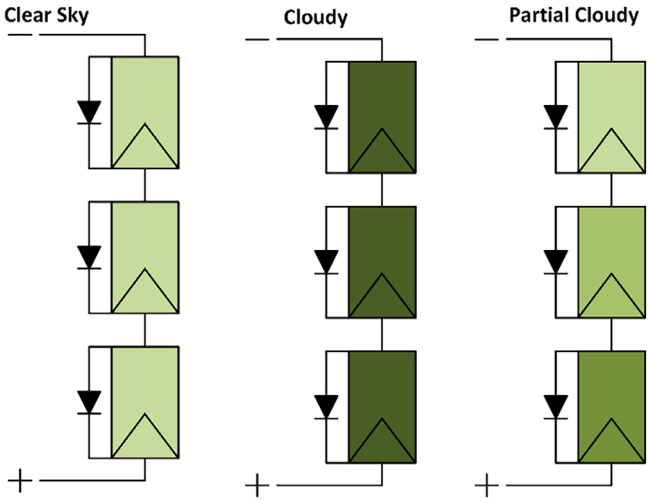


FIGURE 4 Uniform and non-uniform irradiance patterns.

TABLE 2 Weather conditions.

Radiation [W/m^2]	**Temperature [°C]**
1000	55
1000	45
1000	35
1000	25
800	25
600	25
250	25

2.2 | Generating PV model characteristics

Figure 5 shows the *I*–*V* and *V*–*P* curves under STC. The 5PM results are indicated with a blue 'x'. The PVM characteristics were formed for different PV panels under several irradiations and temperatures listed in Table 2.

I–*V* and *P*–*V* curves are shown in Figures 6 and 7. With the decrease in irradiation, I_{SC}, P_{MPP}, and panel current decreased. Namely, I_{MPP} remained almost constant while V_{MPP} decreased.

The *P*–*V* and *I*–*V* characteristics of PVMs under CS, cloudy, and partial cloudy are given in Figure 8. Also, GMPP and local MPPs are indicated by yellow, black, and brown stars. Due to changes in irradiation under cloudy conditions, GMPP can be successfully detected despite the presence of local MPPs.

2.3 | Regression analysis

Regression analysis is the most used method for finding the relationship between two variables in statistical solutions. Regression analysis can be linear or non-linear, depending on the dataset. Thus, linear and non-linear regression analyses were applied to the proposed MPPT to track GMPP in a shorter time and avoid LMPPs. For performing curve fitting, the independent variables were selected as temperature and irradiation, and the dependent variable was chosen as the voltage at MPP [59]. The dataset was formed with the generated PVM characteristics under several weather conditions and used for curve fitting.

The flowchart for the suggested hybrid GMPPT structure is provided in Figure 9. The PVlib library provided in Python generates *P*–*V* and *I*–*V* characteristics of the De Soto PV model. Datasets of irradiation (IR), temperature (*T*), power at MPP (P_{mpp}), and voltage at MPP (V_{mpp}) are created accordingly. Then, regression is started by selecting linear or non-linear regression types according to dataset curves. The data is partially used to train, test, and validate the machine learning model empowered by the regression method. Consequently, linear and non-linear regression equations are derived. P&O-based GMPPT yet can define the search range to find GMPP.

A dataset was created using the PVlib-De Soto under variable weather conditions. The first dataset of V_{mpp} was obtained by changing the irradiance by 20 W/m^2 steps in the range of 150 to 1500 W/m^2 under constant temperature, as shown in Figure 10a. V_{mpp} changes between 16.39 and 21.70 V as the irradiation increases. The second dataset of V_{mpp} was obtained by changing the temperature from −5 to 50°C in 3°C steps under constant irradiation, as given in Figure 10b. V_{mpp} approximately was changed linearly between 20.36 and 24.92 V as temperature increased under constant irradiation. Also, Figure 10 shows the similarity of voltage and power at MPP obtained with the De Soto-5PM. Equations (24) and (25) were obtained from performing curve fitting with linear and non-linear regressions via Python Scikit-learn. Furthermore, a search area was created around the MPP determined by Equation (24) to avoid being stuck at the LMPP. The performance of the model can be measured in terms of root mean square error (RMSE), mean relative error (MRE), mean absolute error (MAE), and absolute error (AE), given in Equations (20) to (23).

$$RMSE\ (\%) = \frac{\sqrt{\frac{\sum_{i=1}^{N}(I_{PVE}-I_{PVM})^2}{N}}}{I_{SC_{PVE}}}\,100 \tag{20}$$

$$MRE\ (\%) = \frac{|X_{PVE}-X_{PVM}|}{X_{PVM}}100 \tag{21}$$

$$MAE = \frac{\sum_{i=1}^{N}|I_{PVE}-I_{PVM}|}{N} \tag{22}$$

$$AE = \max|I_{PVE}-I_{PVM}| \tag{23}$$

17521424, 2024, 9-10, Downloaded from https://ietresearch.onlinelibrary.wiley.com/doi/10.1049/rpg2.13017 by Yildiz Technical University, Wiley Online Library on [19/07/2024]. See the Terms and Conditions (https://onlinelibrary.wiley.com/terms-and-conditions) on Wiley Online Library for rules of use; OA articles are governed by the applicable Creative Commons License

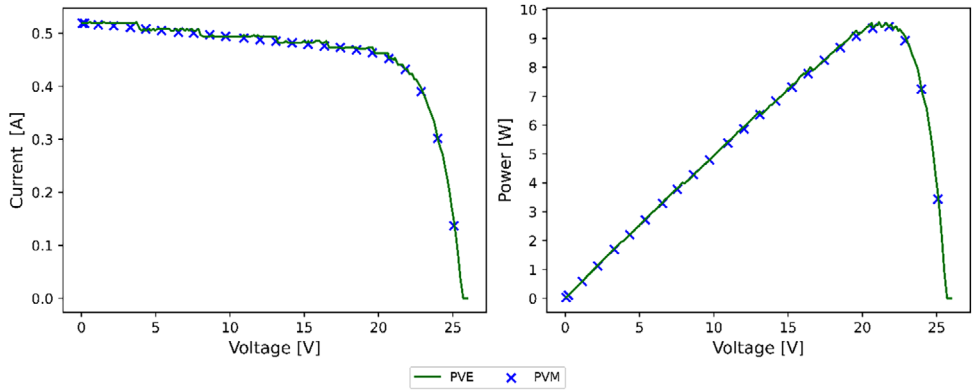


FIGURE 5 *I–V* and *P–V* characteristics of PVM under STC. PVM, photovoltaic models; STC, standard test conditions.

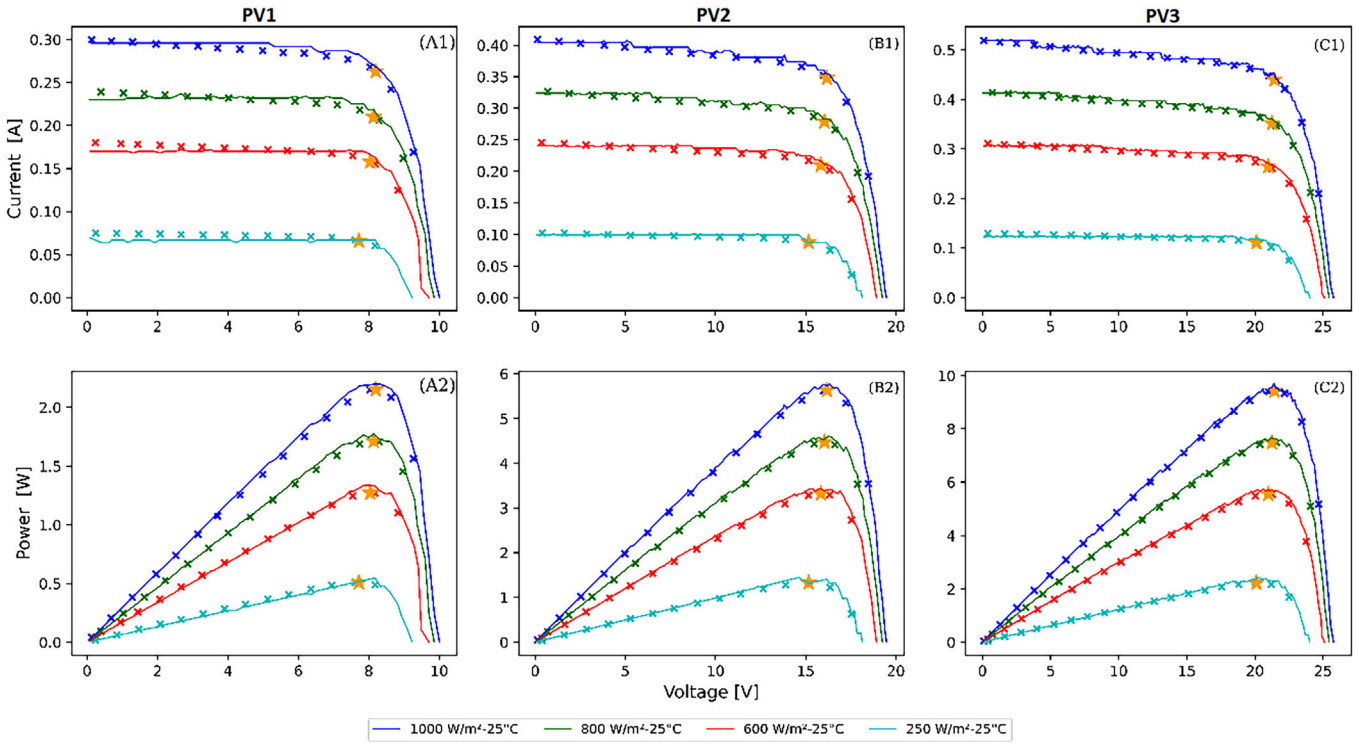


FIGURE 6 *I–V* and *P–V* curves under variable irradiation and constant temperature.

$$V_{mpp}^{lin} = 22.95 + 0.0013330.IR - 0.118.T \tag{24}$$

$$V_{mpp}^{nonlin} = 18.50 - 0.007530.IR^2 - 0.117.T \tag{25}$$

$$V_{mpp}^{min} < V_{mpp}^{search} < V_{mpp}^{max} \tag{26}$$

The blue dots show the dataset used for regression analysis in Figure 11a1. The dashed red line represents the linear regression, and the solid red curve is the non-linear regression in Figure 11a1. The linear regression is Equation (24), and the non-linear regression is Equation (25), where T is temperature, and IR is irradiation. Figure 11a2 shows the effect of temperature variation on V_{mpp}. Figure 11a3 depicts the difference between the predicted and dataset of V_{mpp}. Table 3 shows that the mean error of V_{mpp} is between 0.004 and 0.119 according to the linear and second-order non-linear regression equations. V_{mpp} was determined with an average error rate of 1.4% due to irradiation and temperature change. Therefore, V_{mpp} is detected with re-loops in the search area of ± 2% to avoid possible LMPP as defined in Equation (26). The theoric and experimental performance comparison is given in Table 4 under 1000 W/m^2 and 25°C. The method's maximum and mean current oscillations are 11 and 3.959 mA. RMSE is 0.9394%.

17521424, 2024, 9-10, Downloaded from https://ietresearch.onlinelibrary.wiley.com/doi/10.1049/rpg2.13017 by Yildiz Technical University, Wiley Online Library on [19/07/2024]. See the Terms and Conditions (https://onlinelibrary.wiley.com/terms-and-conditions) on Wiley Online Library for rules of use; OA articles are governed by the applicable Creative Commons License

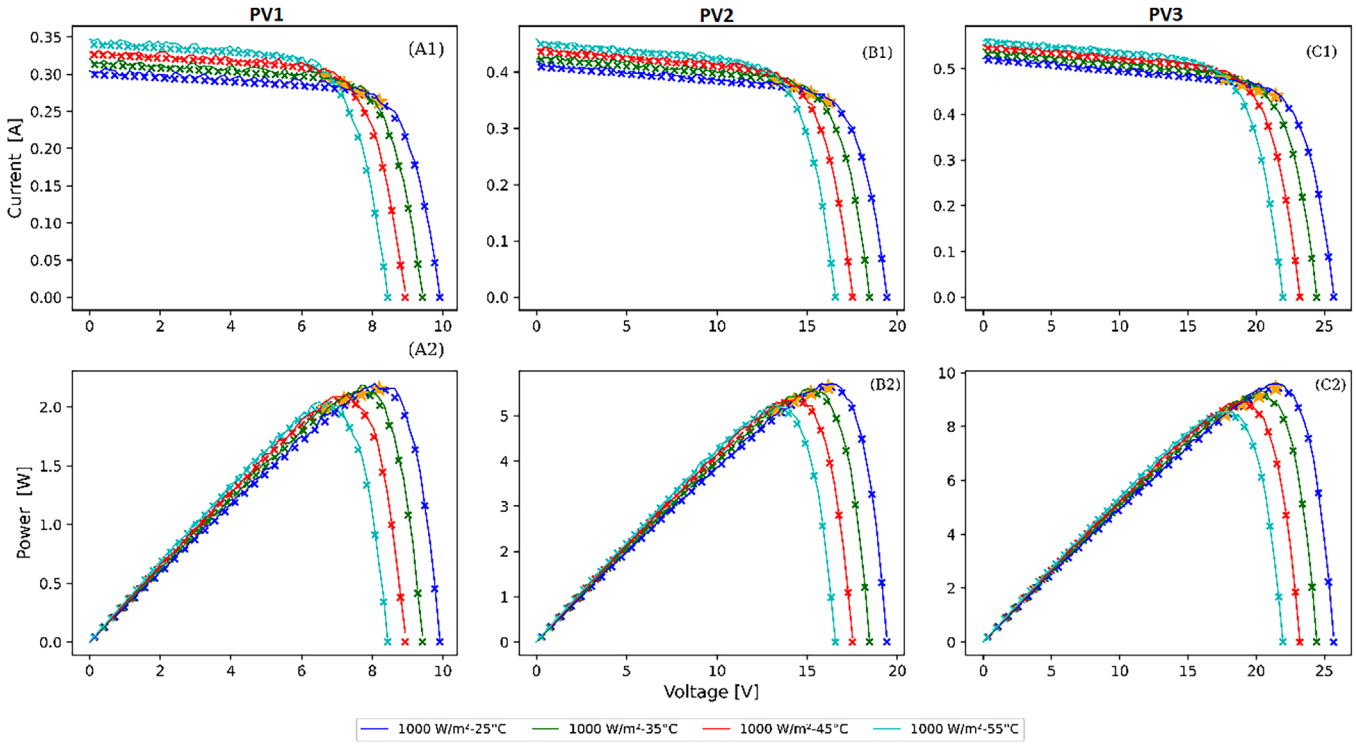


FIGURE 7 *I–V* and *P–V* curves under variable temperature and constant irradiation.

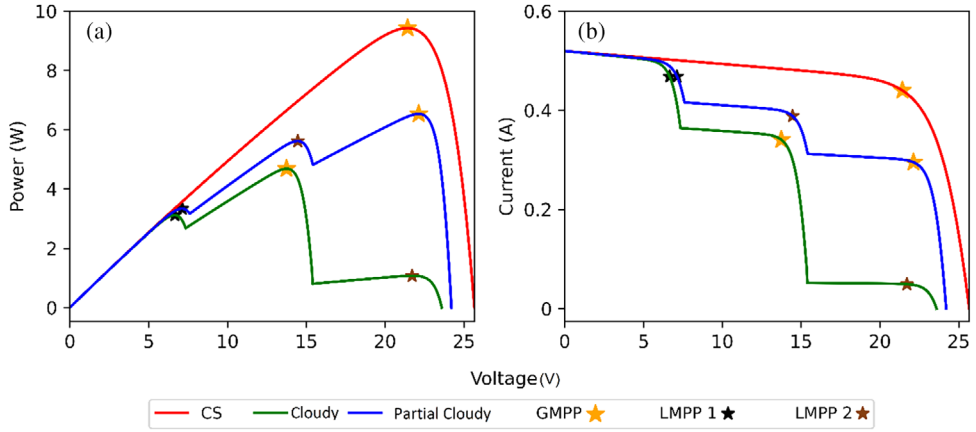


FIGURE 8 (A) *P–V* and (B) *I–V* curves under different partial shading patterns.

2.4 | The suggested hybrid structure

New strategies for building low-cost PV emulators mimics parallel with PV panel are required due to the high cost of commercial counterparts. Therefore, a low-cost PV emulator was designed in this study as shown in Figure 12. It consists of a rectifier, a DC-DC buck converter, a voltage controller, and a current limiter, which are controlled by a microprocessor. This converter can be set either identical or different values of irradiation and temperature. The variable load is used for presenting the resistance of MPPT. Duty ratio of DC–DC buck converter is set by regression-based perturb and observe algorithm running in the Python environment. The PV array and weather data selected by the user are entered into the PVLIB-De Soto PVM. The microcontroller controls the current limiting and voltage regulation circuits with an algorithm. Then, reference values calculated according to PVM were measured at the DC–DC converter output with approximately 1% RMSE (under STCs). In this way, the DC–DC converter can be run as PV emulator (PVE) in different weather conditions. Thanks to the Python environment, the results can be dynamically stored and visualized. The key benefit of the proposed hybrid design lies in its adaptability to simulate varying levels of irradiation and temperature, alongside its straightforward implementation.

17521424, 2024, 9-10, Downloaded from https://ietresearch.onlinelibrary.wiley.com/doi/10.1049/rpg2.13017 by Yildiz Technical University, Wiley Online Library on [19/07/2024]. See the Terms and Conditions (https://onlinelibrary.wiley.com/terms-and-conditions) on Wiley Online Library for rules of use; OA articles are governed by the applicable Creative Commons License

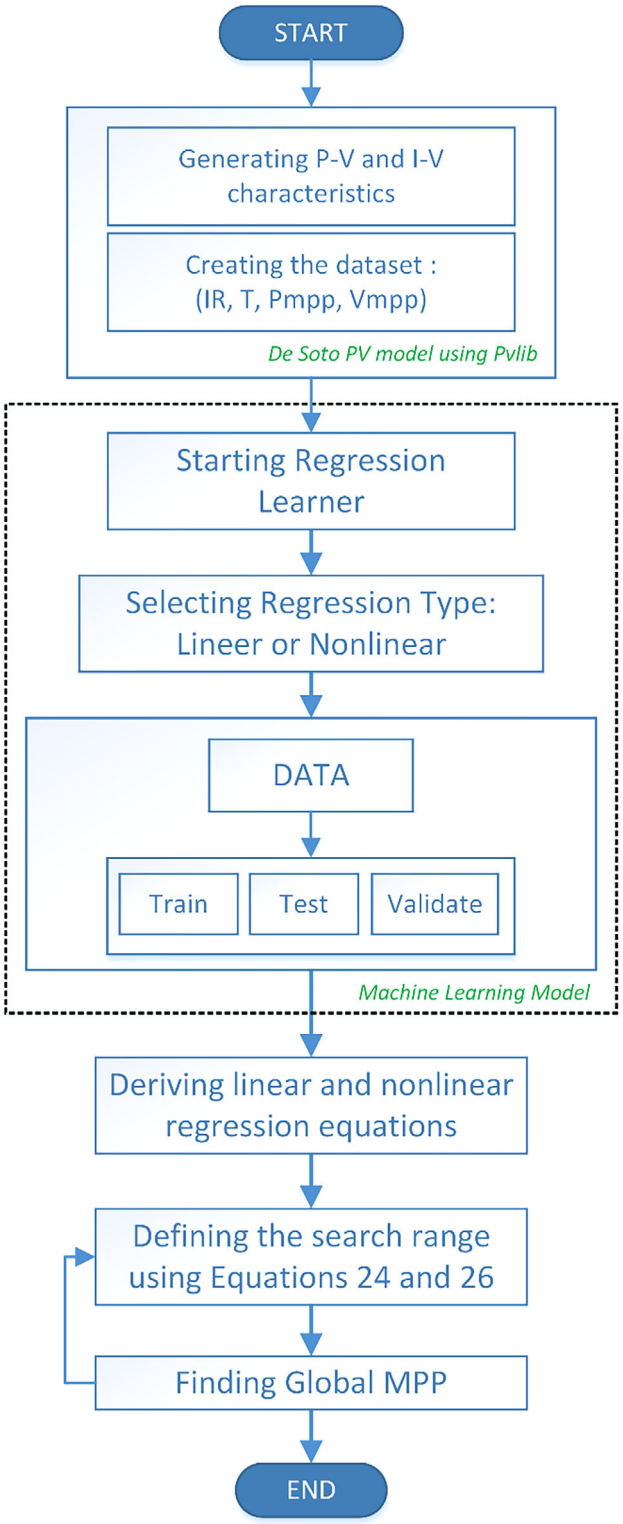


FIGURE 9 The flowchart of the suggested hybrid GMPPT powered by regression. GMPPT, global maximum power point tracker.

The suggested regression-based hybrid structure has been created in Python regarding solar panel parameters and weather data. The experimental setup of the proposed GMPPT is given in Figure 13. The structure has microcontrollers to control the voltage and limit the current. The flowcharts of the voltage controller and current limiter designed for the structure are given in Figure 14.

TABLE 3 Regression errors.

Regression type	Average errors	
	Temperature (const.) Irradiation (variable)	Temperature (variable) Irradiation (const.)
Linear	0.199	0.006
Non-linear (second order)	0.119	0.004

TABLE 4 Theoric and experimental performance comparison under STC.

Parameters	PVM	Experiment	MRE [%]
V_{OC} [V]	25.668	25.96	1.1376
I_{SC} [A]	0.519	0.519	0
P_{MPP} [W]	9.428	9.563	1.43
V_{MPP} [V]	21.424	21.11	1.4656
I_{MPP} [A]	0.44	0.453	2.9545

Abbreviations: MRE, mean relative error; PVM, photovoltaic models; STC, standard test conditions.

The output voltage is zero, and the current is set to I_{SC} to draw the I–V curve. Then, the voltage is increased by one step. If the voltage is less than V_{OC}, the current limiter is started. According to the increased voltage, the current at this voltage is calculated using the I–V relation of PVM. If the current (I_{PV}) is greater than the tolerance of 0.5%, it is reduced by ΔI steps until it is below the tolerance. It is checked every loop. The current and voltage are recorded when the difference is less than the tolerance. After the first I–V curve is completed, the voltage increases one step for the second. The algorithm ends when the output voltage exceeds V_{OC}.

The main flowchart of the suggested hybrid GMPPT algorithm is given in Figure 15. PVMs are created with the panel parameters and weather data. V_{mpp} was approximately determined using Equation (24). Then, V_1–V_2 limits are determined according to Equation (26) within ± 2% to avoid getting stuck in LMPP. Then, the current limiter found P_{LB} for each voltage step in the specified range. This cycle is repeated for each voltage determined by ΔV steps in the V_1–V_2 range. The obtained LMPP in that range is assigned as the global best for iteration i. This process is repeated until all weather data is completed.

3 | EXPERIMENTAL PERFORMANCE RESULT AND DISCUSSION

The results of the improved hybrid method are provided in Table 5. Lower irradiation and power lead to more RMS errors. The maximum power of PV3 decreased approximately linearly with increasing temperature. It has been observed that the relative power loss has increased, especially at temperatures higher than 35°C.

17521424, 2024, 9-10, Downloaded from https://ietresearch.onlinelibrary.wiley.com/doi/10.1049/rpg2.13017 by Yildiz Technical University, Wiley Online Library on [19/07/2024]. See the Terms and Conditions (https://onlinelibrary.wiley.com/terms-and-conditions) on Wiley Online Library for rules of use; OA articles are governed by the applicable Creative Commons License

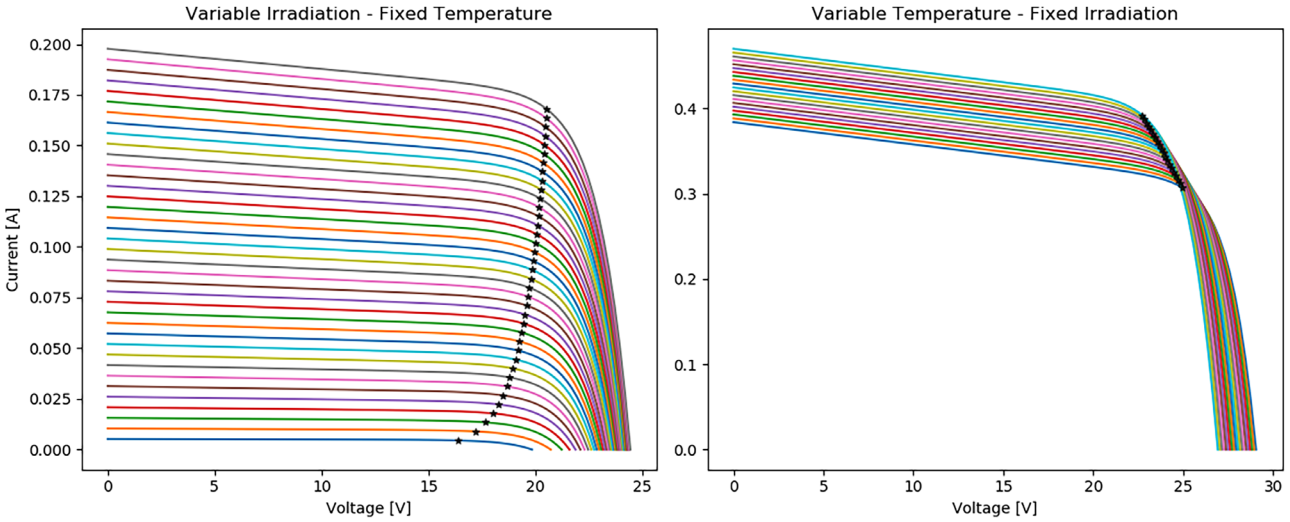


FIGURE 10 Voltage variations under fixed and variable temperature and irradiation.

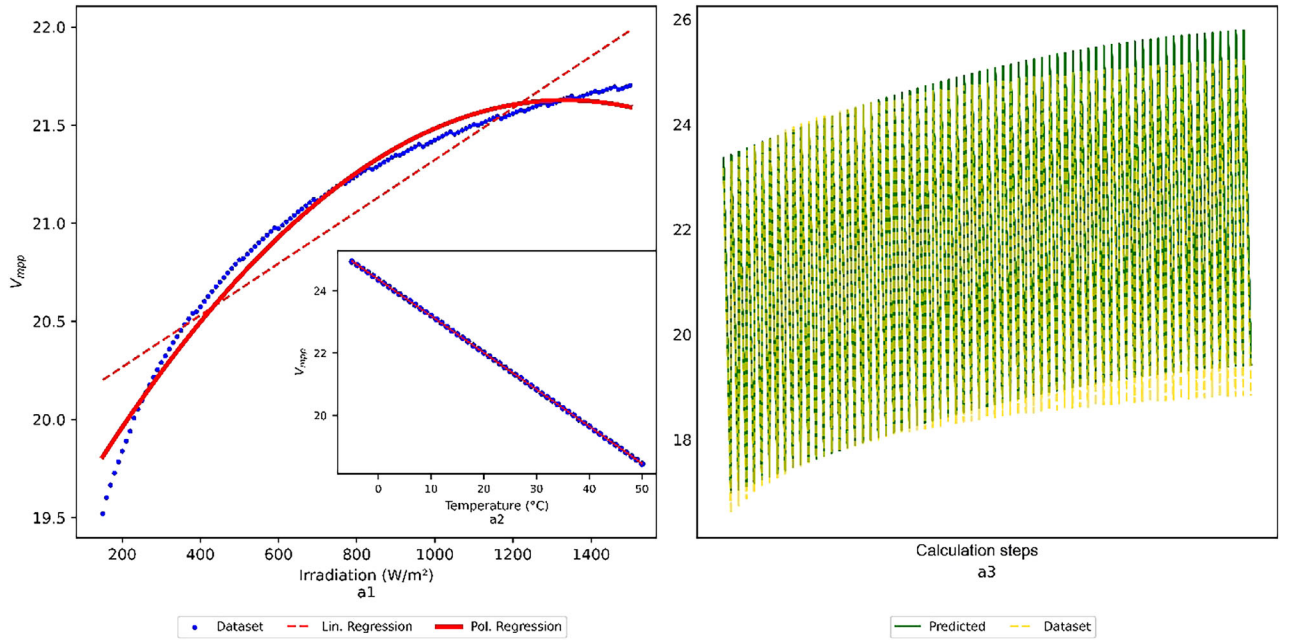


FIGURE 11 Results of linear and regression analyses.

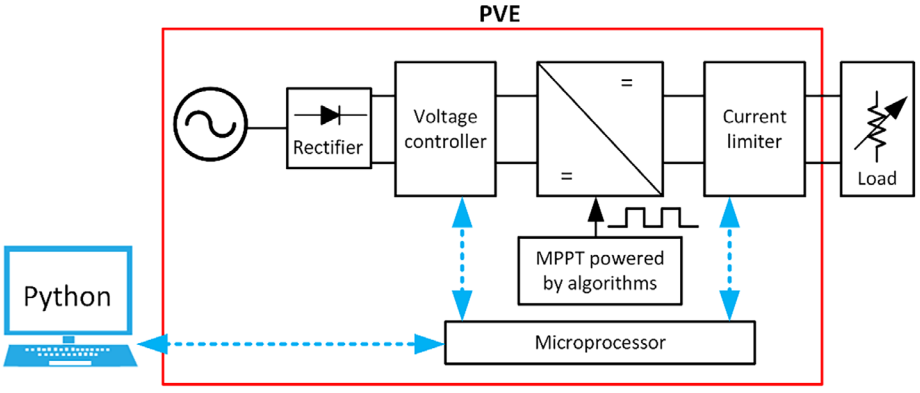


FIGURE 12 GMPPT block diagram [19]. GMPPT, global maximum power point tracker.

17521424, 2024, 9-10, Downloaded from https://ietresearch.onlinelibrary.wiley.com/doi/10.1049/rpg2.13017 by Yildiz Technical University, Wiley Online Library on [19/07/2024]. See the Terms and Conditions (https://onlinelibrary.wiley.com/terms-and-conditions) on Wiley Online Library for rules of use; OA articles are governed by the applicable Creative Commons License

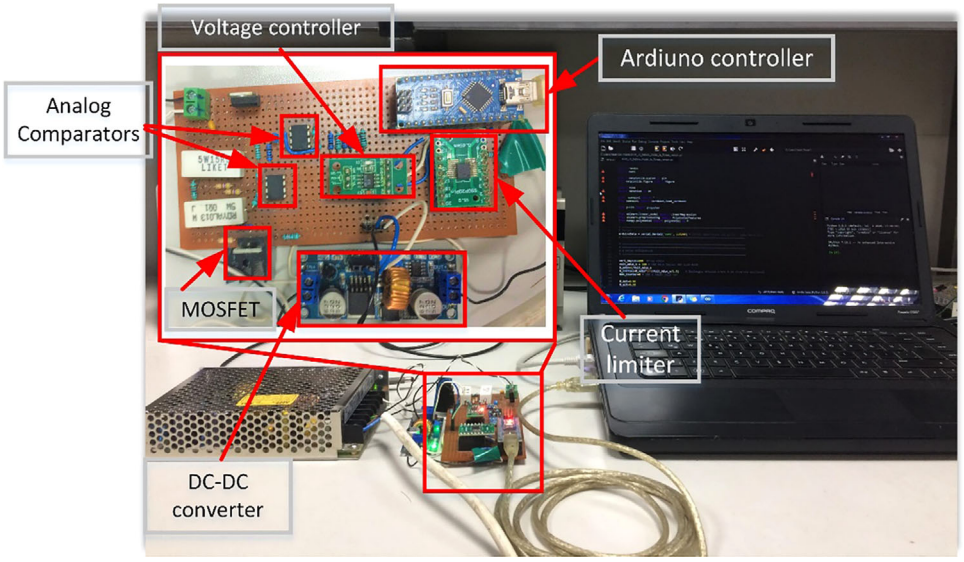


FIGURE 13 The experimental setup for the proposed GMPPT. GMPPT, global maximum power point tracker.

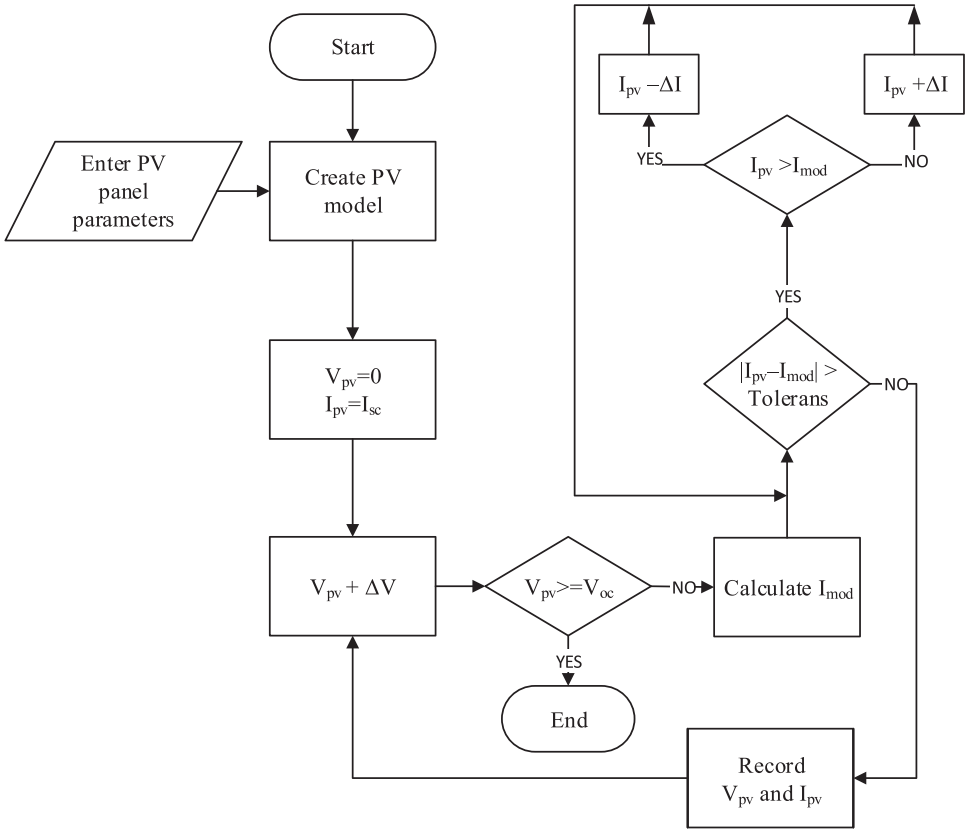


FIGURE 14 The voltage controller and current limiter.

The weather data with 5-min resolution was measured at the Electrical Engineering Building of Yıldız Technical University. The sample days were modelled using the measured weather data and given in Figure 16 to compare the dynamic performance of the proposed GMPPT. Clear sky, cloudy, and partial cloudy days were selected to test the performance of the suggested GMPPT using three different solar panel models. The performance of GMPPT was compared to the generated PVM results for 1 day-long operation and given in Figure 17. The results other than the power output of the suggested GMPPT

17521424, 2024, 9-10, Downloaded from https://ietresearch.onlinelibrary.wiley.com/doi/10.1049/rpg2.13017 by Yildiz Technical University, Wiley Online Library on [19/07/2024]. See the Terms and Conditions (https://onlinelibrary.wiley.com/terms-and-conditions) on Wiley Online Library for rules of use; OA articles are governed by the applicable Creative Commons License

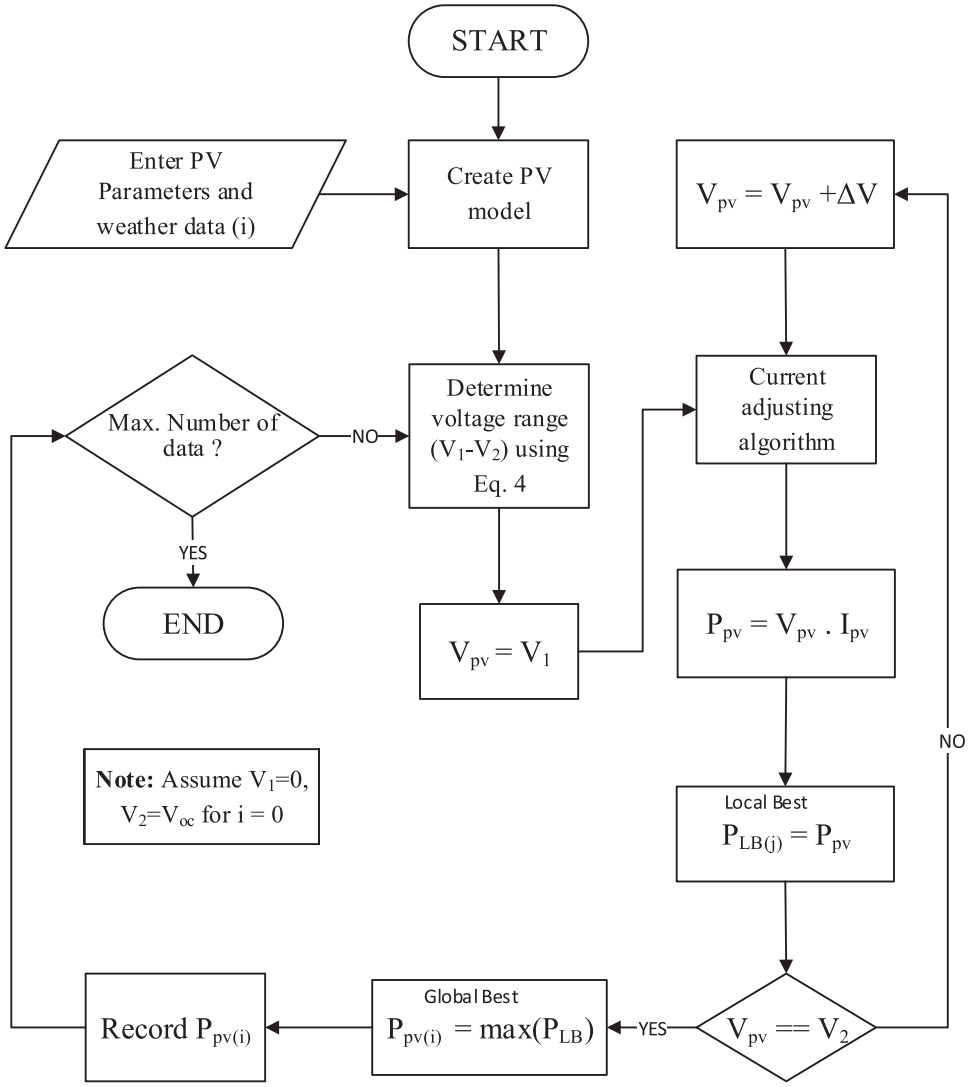


FIGURE 15 The main flowchart of GMPPT. GMPPT, global maximum power point tracker.

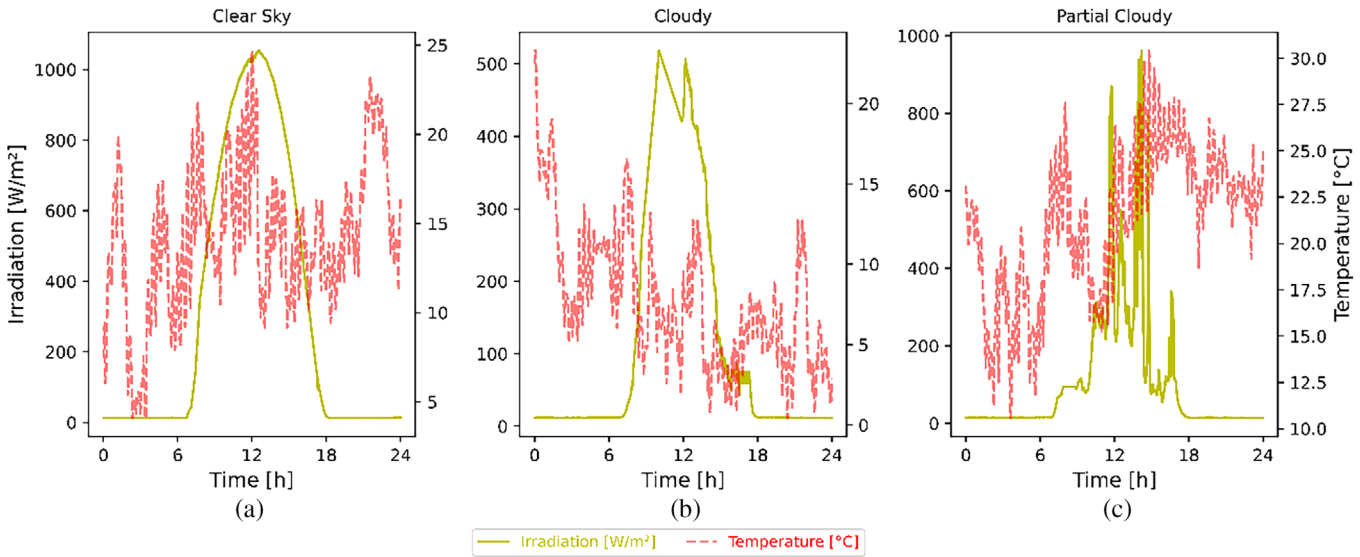


FIGURE 16 Irradiation and temperature under (a) clear sky, (b) cloudy, (c) partial cloudy.

17521424, 2024, 9-10, Downloaded from https://ietresearch.onlinelibrary.wiley.com/doi/10.1049/rpg2.13017 by Yildiz Technical University, Wiley Online Library on [19/07/2024]. See the Terms and Conditions (https://onlinelibrary.wiley.com/terms-and-conditions) on Wiley Online Library for rules of use; OA articles are governed by the applicable Creative Commons License

TABLE 5 Comparison of panels' dynamic results.

			PV3		PV2		PV1	
Irradiation [W/m^2]	**Temp. [°C]**	**Parameters**	**De Soto Model**	**Improved hybrid method**	**De Soto Model**	**Improved hybrid method**	**De Soto Model**	**Improved hybrid method**
1000	25	V_{OC}	25.668	25.77	19.403	19.55	9.914	10.01
		I_{SC}	0.5190	0.519	0.41	0.404	0.3	0.296
		P_{MPP}	9.4280	9.55647	5.635	5.74542	2.154	2.19781
		V_{MPP}	21.424	21.67	16.169	16.23	8.196	8.11
		I_{MPP}	0.440	0.441	0.348	0.354	0.263	0.271
		RMSE	0.962		0.986		1.591	
		AE	0.684		0.406		0.261	
1000	35	V_{OC}	24.431	24.525	18.457	18.472	9.424	9.510
		I_{SC}	0.533	0.536	0.423	0.424	0.313	0.315
		P_{MPP}	9.146	9.195	5.498	5.583	2.115	2.176
		V_{MPP}	20.185	20.210	15.209	15.02	7.683	7.673
		I_{MPP}	0.453	0.455	0.374	0.371	0.275	0.283
		RMSE	0.537		0.220		0.07	
		AE	0.321		0.261		0.194	
1000	45	V_{OC}	23.192	23.185	17.509	17.590	8.932	8.875
		I_{SC}	0.546	0.551	0.436	0.440	0.327	0.335
		P_{MPP}	8.825	8.859	5.333	5.422	2.063	2.126
		V_{MPP}	18.946	19.010	14.265	14.507	7.199	7.273
		I_{MPP}	0.466	0.466	0.374	0.373	0.287	0.292
		RMSE	0.665		0.279		0.106	
		AE	0.340		0.281		0.216	
1000	55	V_{OC}	21.949	21.930	16.558	16.450	8.44	8.498
		I_{SC}	0.560	0.563	0.450	0.458	0.34	0.342
		P_{MPP}	8.467	8.505	5.14	5.204	1.997	2.035
		V_{MPP}	17.71	17.719	13.324	13.246	6.694	6.661
		I_{MPP}	0.478	0.480	0.386	0.392	0.298	0.306
		RMSE	0.811		0.346		0.135	
		AE	0.356		0.290		0.230	

Abbreviations: AE, absolute error; PV, photovoltaic; RMSE, root mean square error.

are provided in Table 6. The accuracy of GMPPT is also evaluated regarding the theoric and experimental energy harvesting and runtime for nine case studies. It is observed that the solar panel obtained the lowest accuracy with the lowest power under partial cloudy conditions. Under cloudy conditions, the absolute error is the same and is about 95% regardless of panel power. Under CS, the accuracy is greater than 98% for all panels. The experimental average absolute errors for PV3, PV2, and PV1 panels are 0.51 under clear sky, 0.658 under cloudy, and 0.77 under partial cloudy.

4 | CONCLUSION

This paper proposes a regression-based Perturb and Observe method to quickly find the global maximum power point avoiding being stuck in local maxima. The proposed method in this study can find global maximum power points and avoid being stuck in LMPPs successfully. Global maximum power point could be detected faster than analytical search algorithm using a flexible Python environment within narrowed search area determined by regressions derived by 5PM. Under cloudy conditions, the absolute error is the same and is about 95% regardless of panel power. Under CS conditions, all panels have an accuracy greater than 98%. The experimental average absolute errors for the PV3, PV2, and PV1 panels are 0.51 under CS, 0.658 under cloudy, and 0.77 under partial cloudy. On the other hand, the accuracy reaches 99% under CS, while it only rises to 95.8% under partial cloudy according to the results of one-day-long real simulation. Additionally, the dynamically recorded results can be visualized to use by developers. The proposed regression-based P&O method is better than its

17521424, 2024, 9-10, Downloaded from https://ietresearch.onlinelibrary.wiley.com/doi/10.1049/rpg2.13017 by Yildiz Technical University, Wiley Online Library on [19/07/2024]. See the Terms and Conditions (https://onlinelibrary.wiley.com/terms-and-conditions) on Wiley Online Library for rules of use; OA articles are governed by the applicable Creative Commons License

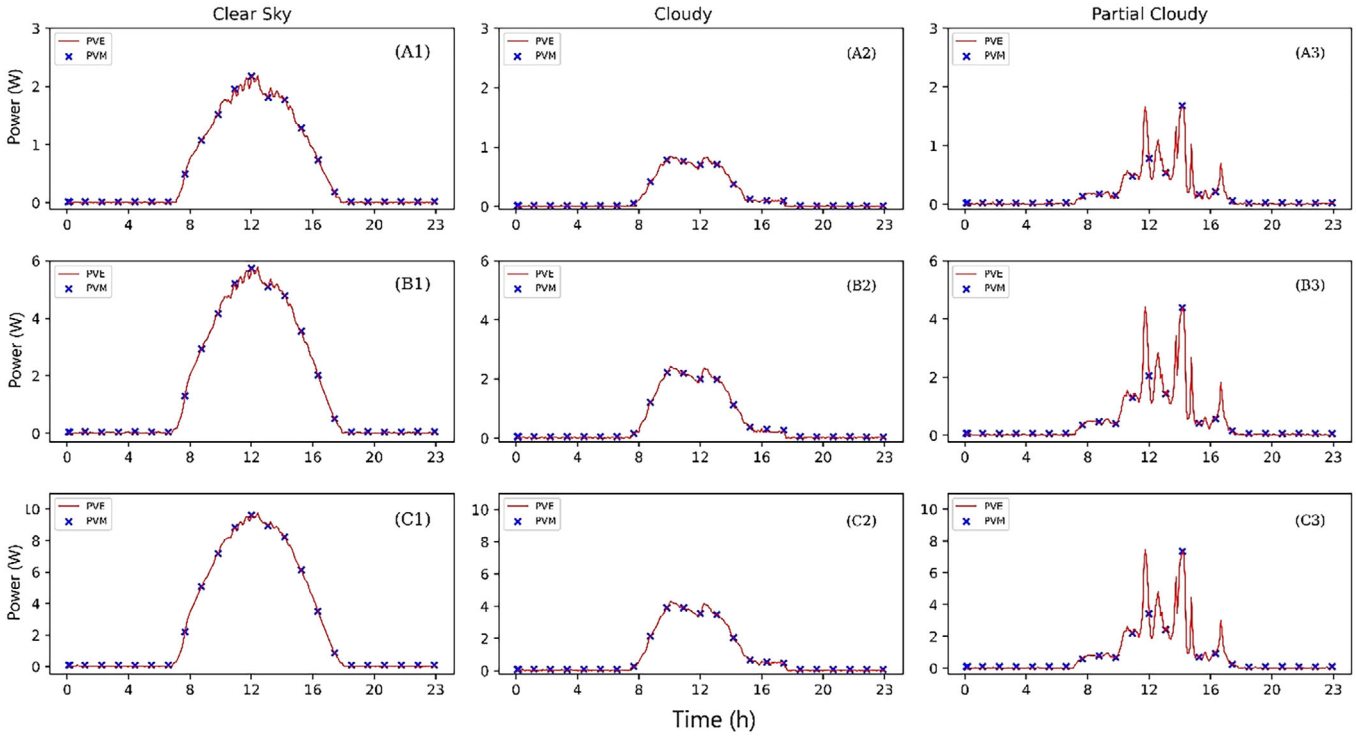


FIGURE 17 Daily power outputs of PVE and PVM. PVM, photovoltaic models.

TABLE 6 Comparison of different panels under uniform and non-uniform weather conditions.

	Panel	Weather	Experimental [Wh]	Theoric (De Soto) [Wh]	Absolute error	Accuracy [%]	Runtime [s]
Case I	PV3	Clear sky	65.869	66.514	0.645	99.030	182.0722
Case II		Cloudy	22.766	23.848	1.082	95.463	170.2983
Case III		Partial Cloudy	20.394	21.768	1.374	93.688	162.1585
Case IV	PV2	Clear sky	38.056	38.662	0.606	98.433	145.0015
Case V		Cloudy	12.762	13.437	0.675	94.977	125.1878
Case VI		Partial Cloudy	12.356	12.898	0.542	95.798	119.6340
Case VII	PV1	Clear sky	13.906	14.193	0.287	97.978	78.5952
Case IIX		Cloudy	4.475	4.692	0.217	95.375	66.6608
Case IX		Partial Cloudy	4.478	4.885	0.407	91.668	72.7302

Abbreviation: PV, photovoltaic.

contemporary counterparts in terms of solution speed, adaptive ability to different weather conditions, the capability of long-term modelling, and higher accuracy. Also, it provides a short learning time and easy implementation to hardware.

AUTHOR CONTRIBUTIONS

Hasan Gundogdu: Investigation; methodology; software; visualization; writing—original draft. **Alpaslan Demirci**: Conceptualization; project administration; supervision; writing—review and editing. **Said Mirza Tercan**: Investigation; methodology; writing—review and editing. **Ali Durusu**: Validation; writing—review and editing.

CONFLICT OF INTEREST STATEMENT

The authors declare no conflict of interest.

FUNDING INFORMATION

The authors received no specific funding for this work.

17521424, 2024, 9-10, Downloaded from https://ietresearch.onlinelibrary.wiley.com/doi/10.1049/rpg2.13017 by Yildiz Technical University, Wiley Online Library on [19/07/2024]. See the Terms and Conditions (https://onlinelibrary.wiley.com/terms-and-conditions) on Wiley Online Library for rules of use; OA articles are governed by the applicable Creative Commons License

DATA AVAILABILITY STATEMENT

Data sharing is not applicable to this article as no new data were created or analyzed in this study.

ORCID

Alpaslan Demirci https://orcid.org/0000-0002-1038-7224
Said Mirza Tercan https://orcid.org/0000-0003-1663-713X
Ali Durusu https://orcid.org/0000-0002-8749-4570

REFERENCES

1. Mahmoodi Tabar, S., Shahnazari, M., Heshmati, K.: Maximum power point tracking in partially shaded photovoltaic systems using grasshopper optimization algorithm. IET Renew. Power Gener. 17(2), 389–399 (2023)
2. Karami, N., Moubayed, N., Outbib, R.: General review and classification of different MPPT techniques. Renew. Sustain. Energy Rev. 68(October 2016), 1–18 (2017)
3. Sarwar, S., Javed, M.Y., Jaffery, M.H., et al.: A novel hybrid MPPT technique to maximize power harvesting from PV system under partial and complex partial shading. Appl. Sci. 12(2), 587 (2022)
4. Hamza Zafar, M., Mujeeb Khan, N., Feroz Mirza, A., et al.: A novel meta-heuristic optimization algorithm based MPPT control technique for PV systems under complex partial shading condition. Sustain. Energy Technol. Assessments 47(June), 101367 (2021)
5. Linus, R.M., Damodharan, P.: Maximum power point tracking method using a modified perturb and observe algorithm for grid connected wind energy conversion systems. IET Renew. Power Gener. 9(6), 682–689 (2015)
6. Cristaldi, L., Faifer, M., Laurano, C., Ottoboni, R., Toscani, S., Zanoni, M.: Model-based maximum power point tracking for photovoltaic panels: Parameters identification and training database collection. IET Renew. Power Gener. 14(15), 2876–2884 (2020)
7. Zakzouk, N.E., Elsaharty, M.A., Abdelsalam, A.K., Helal, A.A., Williams, B.W.: Improved performance low-cost incremental conductance PV MPPT technique. IET Renew. Power Gener. 10(4), 561–574 (2016)
8. Zafar, M.H., Khan, N.M., Mirza, A.F., Mansoor, M.: Bio-inspired optimization algorithms based maximum power point tracking technique for photovoltaic systems under partial shading and complex partial shading conditions. J. Clean. Prod. 309(April), 127279 (2021)
9. Krishnan, G.S., Puthusserry, G.V., Mithun, T., Simon, S.P., Thazhakuni, B.P.: Global maximum power point tracking in partially shaded PV systems using plant reproduction algorithm. IET Renew. Power Gener. 15(4), 903–913 (2021)
10. Javed, S., Ishaque, K.: A comprehensive analyses with new findings of different PSO variants for MPPT problem under partial shading. Ain Shams Eng. J. 13(5), 101680 (2022)
11. Abdulkadir, M., Yatim, A.H.M., Yusuf, S.T.: An improved PSO-based MPPT control strategy for photovoltaic systems. Int. J. Photoenergy 2014, 1–11 (2014)
12. Dagal, I., Akin, B.: Improved particle swarm optimization based on buck-boost converter (IPSO-BBC) for photovoltaic system applications. Recent Adv. Sci. Eng. 2(2), 42–48 (2022)
13. Qais, M.H., Hasanien, H.M., Alghuwainem, S.: Parameters extraction of three-diode photovoltaic model using computation and Harris Hawks optimization. Energy 195, 117040 (2020)
14. Mansoor, M., Mirza, A.F., Ling, Q.: Harris Hawk optimization-based MPPT control for PV systems under partial shading conditions. J. Clean. Prod. 274, 1–19 (2020)
15. Mirjalili, S., Mirjalili, S.M., Lewis, A.: Grey wolf optimizer. Adv. Eng. Softw. 69, 46–61 (2014)
16. Mohanty, S., Subudhi, B., Ray, P.K.: A new MPPT design using grey wolf optimization technique for photovoltaic system under partial shading conditions. IEEE Trans. Sustain. Energy 7(1), 181–188 (2016)
17. Millah, I.S., Chang, P.C., Teshome, D.F., Subroto, R.K., Lian, K.L., Lin, J.-F.: An enhanced grey wolf optimization algorithm for photovoltaic maximum power point tracking control under partial shading conditions. IEEE Open J. Ind. Electron. Soc. 3, 392–408 (2022)
18. Mao, M., Zhang, L., Huang, H., Chong, B., Zhou, L.: Maximum power exploitation for grid-connected PV system under fast-varying solar irradiation levels with modified salp swarm algorithm. J. Clean. Prod. 268, 122158 (2020)
19. Gundogdu, H., Demirci, A., Tercan, S.M., Cali, U.: A novel improved grey wolf algorithm based global maximum power point tracker method considering partial shading. IEEE Access 12, 6148–6159 (2024)
20. Kermadi, M., Salam, Z., Eltamaly, A.M., et al.: Recent developments of MPPT techniques for PV systems under partial shading conditions: A critical review and performance evaluation. IET Renew. Power Gener. 14(17), 3401–3417 (2020)
21. Priyadarshi, N., Maroti, P.K., Khan, B.: An adaptive grid integrated photovoltaic system with perturb T–S fuzzy based sliding mode controller MPPT tracker: An experimental realization. IET Renew. Power Gener. 1–11 (2023)
22. Ali, M.N., Mahmoud, K., Lehtonen, M., Darwish, M.M.F.: Promising MPPT methods combining metaheuristic, fuzzy-logic and ANN techniques for grid-connected photovoltaic. Sensors 21(4), 1244 (2021)
23. Rehman, H., Sajid, I., Sarwar, A., et al.: Driving training-based optimization (DTBO) for global maximum power point tracking for a photovoltaic system under partial shading condition. IET Renew. Power Gener. 17, 2542–2562 (2023)
24. Moghassemi, A., Ebrahimi, S., Padmanaban, S., Mitolo, M., Holm-Nielsen, J.B.: Two fast metaheuristic-based MPPT techniques for partially shaded photovoltaic system. Int. J. Electr. Power Energy Syst. 137(November 2021), 107567 (2022)
25. Xie, Z., Wu, Z.: A flexible power point tracking algorithm for photovoltaic system under partial shading condition. Sustain. Energy Technol. Assessments 49, 101747 (2022)
26. Jiang, Y., Xu, J., Leng, X., Eghbalian, N.: A novel hybrid maximum power point tracking method based on improving the effectiveness of different configuration partial shadow. Sustain. Energy Technol. Assessments 50, 101835 (2022)
27. Priyadarshi, N., Padmanaban, S., Bhaskar, M.S., Azam, F., Khan, B., Hussien, M.G.: A novel hybrid grey wolf optimized fuzzy logic control based photovoltaic water pumping system. IET Renew. Power Gener. 1–12 (2022)
28. Mohanty, S., Subudhi, B., Ray, P.K.: A grey wolf-assisted perturb & observe MPPT algorithm for a PV system. IEEE Trans. Energy Convers. 32(1), 340–347 (2017)
29. Ahmed, J., Salam, Z.: An enhanced adaptive P&O MPPT for fast and efficient tracking under varying environmental conditions. IEEE Trans. Sustain. Energy 9(3), 1487–1496 (2018)
30. Bayarassou, H., Megri, A.F.: New approach based on a fuzzy regression model for a photovoltaic system. Electr. Power Syst. Res. 217, 109091 (2023)
31. Saremi, M., Pourfarzad, H., Nemati, M.: Design of a fuzzy current-sensor less maximum power point tracking algorithm for photovoltaic systems. IET Renew. Power Gener. 14(18), 3724–3731 (2020)
32. Altintaş, N., Yilmaz, A., Demirci, A., Tercan, S.M.: Comparison of maximum power point tracking methods in battery PV systems. Eur. J. Sci. Technol. 2021(31), 369–377 (2021)
33. Padmavathi, N., Chilambuchelvan, A., Shanker, N.R.: Maximum power point tracking during partial shading effect in PV system using machine learning regression controller. J. Electr. Eng. Technol. 16(2), 737–748 (2021)
34. Tan, B., Ke, X., Tang, D., Yin, S.: Improved perturb and observation method based on support vector regression. Energies 12(6), 1151 (2019)
35. Durusu, A., Nakir, I., Ajder, A., Ayaz, R., Akca, H., Tanrioven, M.: Performance comparison of widely-used maximum power point tracker algorithms under real environmental conditions. Adv. Electr. Comput. Eng. 14(3), 89–94 (2014)
36. Nakir, I., Durusu, A., Akca, H., et al.: A new MPPT algorithm for vehicle integrated solar energy system. J. Energy Resour. Technol. 138(2), 021610 (2016)
37. Almeida, M.P., Perpiñán, O., Narvarte, L.: PV power forecast using a nonparametric PV model. Sol. Energy 115, 354–368 (2015)

17521424, 2024, 9-10, Downloaded from https://ietresearch.onlinelibrary.wiley.com/doi/10.1049/rpg2.13017 by Yildiz Technical University, Wiley Online Library on [19/07/2024]. See the Terms and Conditions (https://onlinelibrary.wiley.com/terms-and-conditions) on Wiley Online Library for rules of use; OA articles are governed by the applicable Creative Commons License

38. Batzelis, E.I., Papathanassiou, S.A.: A method for the analytical extraction of the single-diode PV model parameters. IEEE Trans. Sustain. Energy 7(2), 504–512 (2016)
39. Rahman, S.A., Varma, R.K., Vanderheide, T.: Generalised model of a photovoltaic panel. IET Renew. Power Gener. 8(3), 217–229 (2014)
40. Iero, D., Carbone, R., Carotenuto, R., et al.: One-shot SPICE simulation of photovoltaic modules, storage elements, inverter and load. In: 2015 AEIT International Annual Conference (AEIT), IEEE, pp. 1–4 (2015)
41. Ciulla, G., Lo Brano, V., Di Dio, V., Cipriani, G.: A comparison of different one-diode models for the representation of I–V characteristic of a PV cell. Renew. Sustain. Energy Rev. 32, 684–696 (2014)
42. Abdulrazzaq, A.K., Bognár, G., Plesz, B.: Evaluation of different methods for solar cells/modules parameters extraction. Sol. Energy 196(December 2019), 183–195 (2020)
43. Ruschel, C.S., Gasparin, F.P., Krenzinger, A.: Experimental analysis of the single diode model parameters dependence on irradiance and temperature. Sol. Energy 217(October 2020), 134–144 (2021)
44. Merenda, M., Iero, D., Carotenuto, R., Corte, F.G.D.: Simple and low-cost photovoltaic module emulator. Electron 8(12), 1445 (2019)
45. Jordehi, A.R.: Parameter estimation of solar photovoltaic (PV) cells: A review. Renew. Sustain. Energy Rev. 61, 354–371 (2016)
46. Ma, J., Bi, Z., Ting, T.O., Hao, S., Hao, W.: Comparative performance on photovoltaic model parameter identification via bio-inspired algorithms. Sol. Energy 132, 606–616 (2016)
47. Sahu, H.S., Nayak, S.K.: Estimation of maximum power point of a double diode model photovoltaic module. IET Power Electron. 10(6), 667–675 (2017)
48. Elazab, O.S., Hasanien, H.M., Elgendy, M.A., Abdeen, A.M.: Parameters estimation of single- and multiple-diode photovoltaic model using whale optimisation algorithm. IET Renew. Power Gener. 12(15), 1755–1761 (2018)
49. Ram, J.P., Babu, T.S., Dragicevic, T., Rajasekar, N.: A new hybrid bee pollinator flower pollination algorithm for solar PV parameter estimation. Energy Convers. Manag. 135, 463–476 (2017)
50. Kler, D., Goswami, Y., Rana, K.P.S., Kumar, V.: A novel approach to parameter estimation of photovoltaic systems using hybridized optimizer. Energy Convers. Manag. 187(July 2018), 486–511 (2019)
51. Derick, M., Rani, C., Rajesh, M., Busawon, K., Binns, R.: Estimation of Solar Photovoltaic Parameters Using Pattern Search Algorithm. In: Fleming, P., Vyas, N., Sanei, S., Deb, K., (eds.) Springer International Publishing, pp. 184–191 (2017)
52. Hemeida, A.M., Hassan, S.A., Mohamed, A.-A.A., et al.: Nature-inspired algorithms for feed-forward neural network classifiers: A survey of one decade of research. Ain Shams Eng. J. 11(3), 659–675 (2020)
53. Samet, H., Hashemi, F., Ghanbari, T.: Minimum non detection zone for islanding detection using an optimal Artificial Neural Network algorithm based on PSO. Renew. Sustain. Energy Rev. 52, 1–18 (2015)
54. Holmgren, W., Hansen, C., Mikofski, M.: Pvlib python: A python package for modeling solar energy systems. J. Open Source Softw. 3(29), 884 (2018)
55. De Soto, W., Klein, S.A., Beckman, W.A.: Improvement and validation of a model for photovoltaic array performance. Sol. Energy 80(1), 78–88 (2006)
56. Lo Brano, V., Orioli, A., Ciulla, G., Di Gangi, A.: An improved five-parameter model for photovoltaic modules. Sol. Energy Mater. Sol. Cells 94(8), 1358–1370 (2010)
57. Hadj Arab, A., Chenlo, F., Benghanem, M.: Loss-of-load probability of photovoltaic water pumping systems. Sol. Energy 76(6), 713–723 (2004)
58. De Blas, M.A., Torres, J.L., Prieto, E., García, A.: Selecting a suitable model for characterizing photovoltaic devices. Renew. Energy 25(3), 371–380 (2002)
59. Karabinaoğlu, M.S., Çakır, B., Başoğlu, M.E., Kazdaloğlu, A., Güneroğlu, A.: Comparison of deep learning and regression-based MPPT algorithms in PV systems. Turkish J. Electr. Eng. Comput. Sci. 30(6), 2319–2338 (2022)

How to cite this article: Gundogdu, H., Demirci, A., Tercan, S.M., Durusu, A.: An improved regression-based perturb and observation global maximum power point tracker methods. IET Renew. Power Gener. 18, 1646–1660 (2024). https://doi.org/10.1049/rpg2.13017

17521424, 2024, 9-10, Downloaded from https://ietresearch.onlinelibrary.wiley.com/doi/10.1049/rpg2.13017 by Yildiz Technical University, Wiley Online Library on [19/07/2024]. See the Terms and Conditions (https://onlinelibrary.wiley.com/terms-and-conditions) on Wiley Online Library for rules of use; OA articles are governed by the applicable Creative Commons License